2019

Decompression of hydrogen-natural gas mixtures in high-pressure pipelines: CFD modelling using different equations of state

Bin Liu
Shijiazhuang Tiedao University, bl987@uowmail.edu.au

Xiong Liu
University of Wollongong, xiong@uow.edu.au

Cheng Lu
University of Wollongong, chenglu@uow.edu.au

Ajit R. Godbole
University of Wollongong, agodbole@uow.edu.au

Guillaume Michal
University of Wollongong, gmichal@uow.edu.au

See next page for additional authors

Decompression of hydrogen-natural gas mixtures in high-pressure pipelines: CFD modelling using different equations of state

Abstract

When designing high-pressure gas pipelines, it must be ensured that a running fracture is arrested within the shortest possible length. The semi-empirical Battelle Two-Curve Model (BTCM) proposed in the early 1970s is still widely used in the industry to estimate the required toughness of the pipe wall material. The BTCM method requires accurate prediction of the gas decompression wave speed. In this paper, a Computational Fluid Dynamics (CFD) model is proposed to predict the decompression wave speed of high-pressure Hydrogen-Natural Gas (H2NG) mixtures in pipelines. The CFD model is validated against experimental data. Three Equations of State (EOS): the Peng-Robinson (PR) EOS, the AGA8 EOS and the GERG-2008 EOS, are incorporated into the CFD code to estimate the physical properties of the mixtures. The ability of the three EOS to predict the decompression wave speed is evaluated by comparing the predicted results against experimental data. Also, the influence of H 2 fraction in the H2NG mixture on the decompression wave speed is investigated.

Disciplines

Engineering | Science and Technology Studies

Publication Details

Liu, B., Liu, X., Lu, C., Godbole, A., Michal, G. & Teng, L. (2019). Decompression of hydrogen-natural gas mixtures in high-pressure pipelines: CFD modelling using different equations of state. International Journal of Hydrogen Energy, 44 (14), 7428-7437.

Authors

Bin Liu, Xiong Liu, Cheng Lu, Ajit R. Godbole, Guillaume Michal, and Lin Teng

Decompression of hydrogen—natural gas mixtures in high-pressure pipelines: CFD modelling using different equations of state

Bin Liu[a], Xiong Liu[b], Cheng Lu[b, *], Ajit Godbole[b], Guillaume Michal[b], Lin Teng[b, c]

[a] Shijiazhuang Tiedao University, Shijiazhuang 050043, China

[b] School of Mechanical, Materials, Mechatronic and Biomedical Engineering, University of Wollongong, NSW 2522, Australia

[c] Shandong Provincial Key Laboratory of Oil & Gas Storage and Transportation Security, China University of Petroleum (East China), Qingdao 266555, China

Abstract

When designing high-pressure gas pipelines, it must be ensured that a running fracture is arrested within the shortest possible length. The semi-empirical Battelle Two-Curve Model (BTCM) proposed in the early 1970s is still widely used in the industry to estimate the required toughness of the pipe wall material. The BTCM method requires accurate prediction of the gas decompression wave speed. In this paper, a Computational Fluid Dynamics (CFD) model is proposed to predict the decompression wave speed of high-pressure Hydrogen-Natural Gas (H2NG) mixtures in pipelines. The CFD model is validated against experimental data. Three Equations of State (EOS): the Peng-Robinson (PR) EOS, the AGA8 EOS and the GERG-2008 EOS, are incorporated into the CFD code to estimate the physical properties of the mixtures. The ability of the three EOS to predict the decompression wave speed is evaluated by comparing the predicted results against experimental data. Also, the influence of H_2 fraction in the H2NG mixture on the decompression wave speed is investigated.

Keywords: Pipeline; Hydrogen—natural gas mixture; Fracture control; Decompression; CFD modelling

* Corresponding author. Tel.: +61-2-4221-4639; Fax: +61-2-4221-5474.
E-mail address: chenglu@uow.edu.au (C. Lu).

1. Introduction

Hydrogen (H_2) is commonly seen as a sustainable energy source of the future. Widespread use of H_2 will require development of efficient H_2 production without significant CO_2 production, such as using nuclear power [1]. Also, such use will have to be implemented in stages using existing Natural Gas (NG) distribution systems to convey blends of Hydrogen and Natural Gas (H2NG), instead of building specific pipelines for H_2 delivery [2, 3]. In such applications, transportation of H2NG from production site to the end-user will form an important link in the infrastructure. H_2 itself is most commonly transported either by trucks or through pipelines. To transport large quantities of H_2 or H2NG blends over long distances, pipeline transmission appears to be the most efficient and economical way.

Research on H2NG systems has attracted increasing attention in recent years. In Ref. [4, 5], the influence of injection of H_2 into NG pipelines was investigated. It was reported that injection of up to 10% of H_2 by volume will not necessitate any modification of the current NG infrastructure. However, if the fraction of H_2 exceeds 10%, the measuring instruments, control stations and gas transmission equipment such as compressors will need to be changed. Apart from the issues in the transportation, end-user (domestic and industrial) systems using the new blends have attracted great attention as well. Some researchers, e.g. [6-8] have investigated the application of H2NG as a fuel in internal combustion engines. Capocelli and De Falco [9] have pointed out that transportation of H_2 using existing NG gas infrastructure will eventually bring economic benefits.

Among the numerous technical and social issues involved in the transportation of H2NG blends using existing NG pipelines, the safety issue is the most important. Both NG and H_2 are highly flammable. Therefore, any release of H2NG from the pipelines may have catastrophic consequences. There have been a number of studies on risk assessment of NG pipelines [10-15]. However, as the introduction

of H_2 into NG may affect the physical properties of the fluid significantly, further studies are necessary to ensure the safe operation of H2NG pipelines.

In the risk assessment of pipelines, one major concern is the risk posed by a running fracture in the pipe wall resulting from pipeline damage. Under operational conditions, it is very important that a crack, if initiated, does not develop into a running fracture, and is arrested as soon as possible. Fracture control of gas pipelines traditionally uses the semi-empirical Battelle Two-Curve Model (BTCM) [16, 17]. The purpose is to obtain the required toughness of the pipe material for the arrest of a propagating fracture. This graphical method involves the superposition of two independently obtained curves: the gas decompression wave speed curve and the fracture propagation speed curve.

Fig. 1 illustrates the principle of the BTCM qualitatively. In Fig. 1, the red solid line represents the decompression wave speed of the fluid, while the black lines (Curve 1 to Curve 3) are the fracture propagation speed curves for materials with different toughness values. When there is an intersection between a decompression wave speed curve and a fracture propagation curve (e.g. curve 3 with the decompression wave speed curve), the crack is propagated at the same speed as that of the fluid decompression wavefront. Therefore, the pressure at the crack tip will be maintained at the value corresponding to the point of intersection, resulting in further tearing of the pipe material. This amounts to a failure in arresting a running fracture. Ideally, the pipe material should be chosen so as to avoid such intersection (e.g. curve 1 in Fig. 1). In this case, the decompression wave propagates faster than the fracture. Therefore, the pressure at the crack tip will be much lower, which prevents the pipe material from further tearing. The minimum toughness required for the pipe material to avoid the fracture propagation is that the fracture propagation speed curve is tangent to the decompression wave speed curve, e.g. ‘Curve 2’ in Fig. 1.

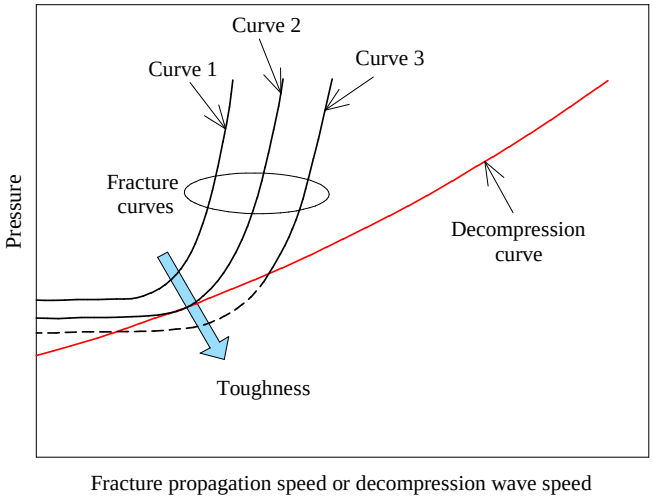

Fig.1 Fracture or decompression wave speed vs Pressure

The fracture propagation speed is usually derived from an analysis of plastic wave propagation, which is semi-empirical through its calibration of fracture resistance:

$$V_f = c\frac{\bar{\sigma}}{\sqrt{R}}\left(\frac{P}{P_a}-1\right)^{\alpha} \tag{1}$$

$$R = \frac{C_V}{A_C} \tag{2}$$

$$P_a = \frac{2\bar{\sigma}t}{3.33\pi r}\arccos\left(e^{-\left(\frac{\pi BRE}{24\sqrt{rt}\bar{\sigma}^2}\right)}\right) \tag{3}$$

where V_f is the fracture propagation speed, $\bar{\sigma}$ is the flow stress, P is the operating pressure, P_a is the arrest pressure, R is the specific Charpy V-Notch (CVN) toughness, C_V is the CVN toughness (energy), A_C is the cross-sectional area of the CVN specimen, r is the pipe diameter, t is the pipe wall thickness, E is the Young's modulus of the pipe material, and C and α are empirical constants.

To obtain a better understanding of the decompression behaviour of gas pipelines, a number of experiments have been conducted in the recent decades. Several full-scale burst tests of NG pipelines have been performed by the European Pipeline Research Group (EPRG), the British Gas Corporation,

Centro Sviluppo Materiali (CSM), and the Battelle Institute [18-22]. However, a full-scale burst test is usually very costly to set up. Alternatively, a small-scale 'shock tube' test can also be used to study the gas decompression characteristics [10, 11, 23-27] in an economical and efficient way. More importantly, due to the much lower cost, different compositions of the gas mixture and various combinations of initial fluid pressure and temperature can be chosen in shock tube experiments to generate sufficient data for model validation.

In the last several decades, a number of numerical models have been developed for the prediction of the gas decompression wave speed, such as GASDECOM [28], DECOM [29], EPDECOM [30], DECAY [31], by Picard and Bishnoi [32, 33], PipeTech [34, 35] and CFD-DECOM [36]. These models are mostly based on one dimensional axial flow theory and were originally proposed for the evaluation of the decompression wave speed of hydrocarbons. The major difference in these models is the use of different Equations of State (EOS). It is obvious that an accurate estimate of the decompression wave speed requires a precise EOS.

Some researchers have compared the performance of various EOS in predicting the decompression wave speed in gas pipelines. Li and Yan [37] compared the specific volumes of binary CO_2 mixtures assuming vapour-liquid equilibrium (VLE), as obtained using several EOS with those obtained from experiments. The binary mixtures consisted of CO_2 mixed with CH_4, H_2S, SO_2, Ar or N_2. Botros [38] predicted the sonic speeds of various hydrocarbon mixtures applying five different EOS: GERG-2008 [39], AGA-8 [40], BWRS [41], PR [42] and SRK [43]. The obtained results were compared with the experimental data from 42 shock tube tests. It was found that the GERG-2008 EOS outperformed the others for pressures up to 30 MPa and temperatures greater than -8°C. Cosham et al. [26] evaluated the decompression wave speeds of pure CO_2 and CO_2 mixtures using different EOS (Span and Wagner [44], GERG, BWRS[41] and PR[42]). It was found that PR EOS predicted a lower saturated liquid density in the critical region than that predicted by the Span and Wagner EOS and the BWRS

EOS for pure CO_2. For CO_2 binary mixtures that include N_2 and CH_4, the trends in the results of both BWRS and GERG EOS are identical. Botros et al. [45-47] compared the decompression wave speeds for pure CO_2 and CO_2 mixture predicted by the GERG-2008 EOS and the PR EOS with those obtained from experiment. It was found that the GERG-2008 EOS shows much better overall performance than the PR EOS. In all of these tests, H_2 or Ar was used as a major component in the binary mixtures, which was previously shown to cause poor performance of both the GERG-2008 and the PR EOS. Richter et al. [48] measured the density of three H_2-enriched natural gas mixtures with H_2 fraction varying from 5% to 30%. Comparison with the results estimated by the GERG-2008 and AGA8 EOS showed that higher H_2 fraction may result in larger prediction error. Hernández-Gómez et al. [49] also measured the density of H_2-enriched NG at temperatures between 260 K and 350 K and pressures up to 20 MPa, for the evaluation of the performance of EOS. It was found that the AGA8-DC92 EOS can produce slightly better prediction than the GERG-2008 EOS for the 13-component H_2-enriched NG, and both the AGA8-DC92 and GERG-2008 EOS provided satisfactory estimates. Studies estimating the other thermodynamic properties of H2NG, such as heat capacity and speed of sound etc. are relatively scarce. To date, no EOS is proposed specifically for H2NG mixtures. Thus, the reliability of different EOS in the prediction of decompression characteristics of H2NG mixtures needs to be investigated.

The purpose of this study is to evaluate the reliability of different EOS for the prediction of decompression wave speed in H2NG pipelines and to evaluate the influence of H_2 fraction on the decompression behaviour. A Computational Fluid Dynamics (CFD) model for a full-bore rupture of a H2NG shock tube is proposed. Three EOS – PR, AGA8 and GERG-2008 were incorporated into the CFD code using a 'real gas' model to predict the physical properties of the fluid. The results were validated against experimental data from shock tube tests. The performances of different EOS were evaluated. Also, simulations were carried out to evaluate the influence of H_2 fraction in the H2NG mixtures on the decompression wave speed using what appears to be the optimal EOS.

2. Methodology

2.1. Computational domain and boundary conditions

The commercially available CFD software ANSYS Fluent (ver. 14.5) was used. The physical flow domain in the shock tube test consists of the volume occupied by the compressed fluid in a horizontal 'shock tube'. The tube is subjected to a 'full-bore' opening at one end using a rupture disc as schematically depicted in Fig.2. It should be noted that a small leakage on the pipeline may not result in a propagating fracture. However, a large crack on the pipeline is highly likely to lead to a propagating fracture and a complete decompression of the fluid in the pipe. If this happens on a large scale, the loss of containment of the pipe may have catastrophic consequences. This study focused on the latter case. Thus a full-bore rupture was considered to investigate the decompression behaviour. Because the depressurisation time during a shock tube test is usually very short, the effect of gravity and heat transfer between the wall and the fluid could be neglected. Accordingly, a two-dimensional (axisymmetric) computational domain was used to reduce the computing time.

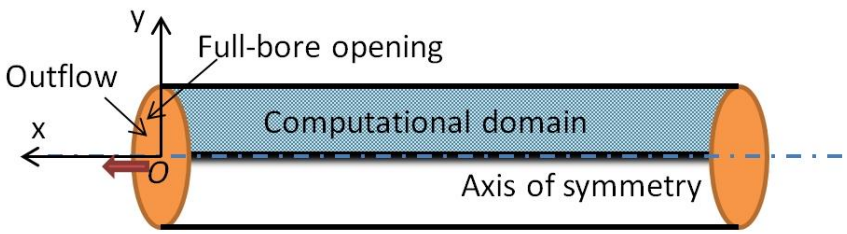

Fig. 2 Schematic of a shock tube (the cylinder) and the computational domain (blue rectangle)

The computational domain was set up according to the dimensions of the shock tube used in the test. On the axis of symmetry, an 'axis' boundary condition was defined. At the rupture end (x = 0), a pressure outlet was specified with ambient pressure and temperature. The closed end and the internal wall of the tube were defined as 'no-slip', adiabatic walls.

Fig. 3 shows a part of the mesh near the rupture end in detail. To ensure that the results are not sensitive to the computational grid, a grid-independence study was carried out in advance. In the employed mesh, the cells immediately adjacent to the boundaries were set at 1 mm from the wall with a growth factor of 1.2. Following the 9th and 4th cell in the axial and radial directions, the dimensions of the cells in the axial and radial directions were maintained at 2 and 5 mm respectively.

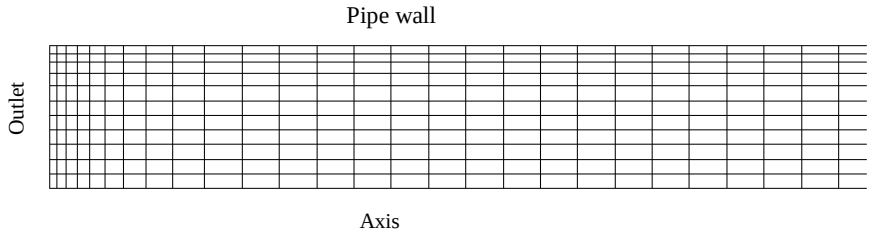

Figure 3 Mesh near the outlet

2.2. Thermodynamic property modelling

To enable accurate modelling of gas decompression, advanced EOS are required to calculate the thermodynamic properties of the fluid over a wide pressure range. In ANSYS Fluent, it is possible to use User Defined Functions (UDFs) to incorporate 'real gas' EOS [16, 50]. Although ANSYS Fluent provides some built-in real gas EOS such as PR, they cannot be directly applied to gas mixtures. To overcome this problem, a User-Defined Real Gas Model (UDRGM) supported by ANSYS Fluent, and which can be implemented through UDFs [51] was developed. In the UDRGM, the thermodynamic properties of the fluid can be calculated at given pressure and temperature at runtime using a real gas EOS. In this study, the physical properties of the fluid were estimated using three real gas EOS: PR, AGA8 and GERG-2008 in the UDRGM.

3. Results and discussion

Three shock tube tests conducted by Botros et al. at the TransCanada Pipeline Gas Dynamic Test Facility [10, 25] were simulated using the proposed CFD model. The main section of the shock tube was a 42 m long 'smooth' pipe, with an Internal Diameter (ID) of 15 inches. The mixtures used in the tests consisted of NG with H_2 fraction ranging from 0% to 8.28%.

During the simulations, the pressure was monitored at a number of locations near the open end of the shock tube, corresponding to the locations where the pressure sensors were installed in the experiment. The locations of the pressure transducers in these tests are presented in Table 1.

A pipeline rupture will result in a leading decompression wavefront travelling away from the rupture plane towards the undisturbed compressed fluid at nearly sonic speed. In the wake of the leading decompression wavefront, the decompression wave speed W is defined in terms of the sonic speed and the 'outflow' velocity, as shown in Eq. (4) [16]:

$$W = c - u \tag{4}$$

where c and u are the sonic speed and 'outflow' velocity, respectively.

In the experiment, the decompression wave speed is not measured directly. However, it can be calculated using time histories of the pressures recorded at known locations on the pipe wall. Usually, after the experiment, the decompression wave speed is calculated by:

$$W = \frac{\mathrm{d}x}{\mathrm{d}t} \tag{5}$$

where x is the distance from the pipe exit and t the time.

According to the method used in the experiment, the decompression wave speed in the simulations was also calculated by Eq. (5) at the locations of the pressure probes as used in the experiment (PT1, PT1A, PT1B, PT2 and PT3).

Table 1 The locations of pressure transducers

Location	Distance from rupture disc (m)
PT1	0.0295
PT1A	0.0924
PT1B	0.1028
PT2	0.2
PT3	0.35
PT4	0.5
PT5	0.7
PT6	0.9
PT7	1.1
PT8	3.1
PT9	5.1
PT10	7.1
PT11	9.1

3.1. Performance evaluation of different EOS

In this study, the decompression of H2NG gas was predicted using three EOS: GERG-2008, AGA8 and PR. 'Test 1' as described by Botros et al. [25] was modelled. In this test, the initial pressure and temperature were 11.947 MPa and 286.18 K respectively. The composition of the mixture was: 93.908% CH_4, 0.099% C_2H_6, 0.146% C_3H_8, 0.214% CO, 2.88% H_2, 0.548%N_2, and 2.205% CO_2.

Fig. 4 compares the pressure histories as predicted by the different EOS against experimental measurements. Ideally, at time $t = 0$, the tube is suddenly opened to the atmosphere as the rupture disc 'disappears'. However, in the experiment, the actual start time of rupture is more likely a little delayed. Therefore, it was considered reasonable to set '$t = 0$' at the instant when the decompression wave arrives at the location of the first pressure sensor (PT1).

It can be seen from the experiment that the pressure experiences an initial sharp drop and then reaches a relatively stable plateau. Clearly, the plateaus predicted by all three EOS are a little lower than those obtained experimentally. For locations farther from the rupture, the duration of the initial sharp drop becomes relatively longer, and the stable plateau is relatively higher. Clearly, the trend and the shape of the pressure drop is successfully captured by the model using the different EOS. The time when the pressure begins to drop at each location, which represents the time that decompression wave reaches the location, is well predicted by the different EOS. Also, the predicted decompression wave arrival time is very close to the measured. The measured and predicted decompression wave arrival times at each sensor location are shown in Table 2. It can be seen that, at most locations the predicted decompression wave arrival times are slightly earlier than the measured, except at PT1A. For most cases, the deviation of this time predicted by the model with GERG-2008 EOS is smaller than those with the other two EOS. Therefore, in this respect, the GERG-2008 EOS seems to be marginally superior to PR and AGA8.

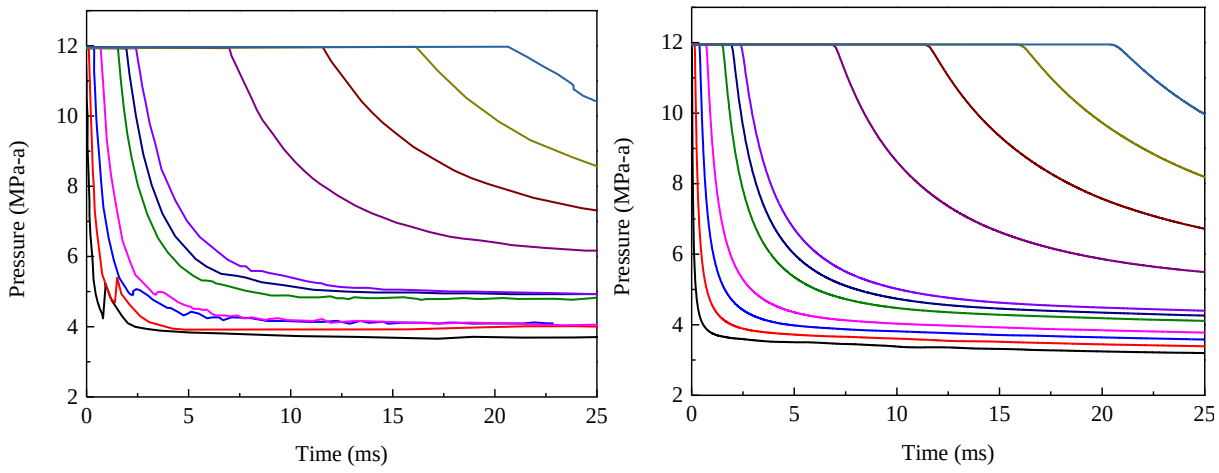

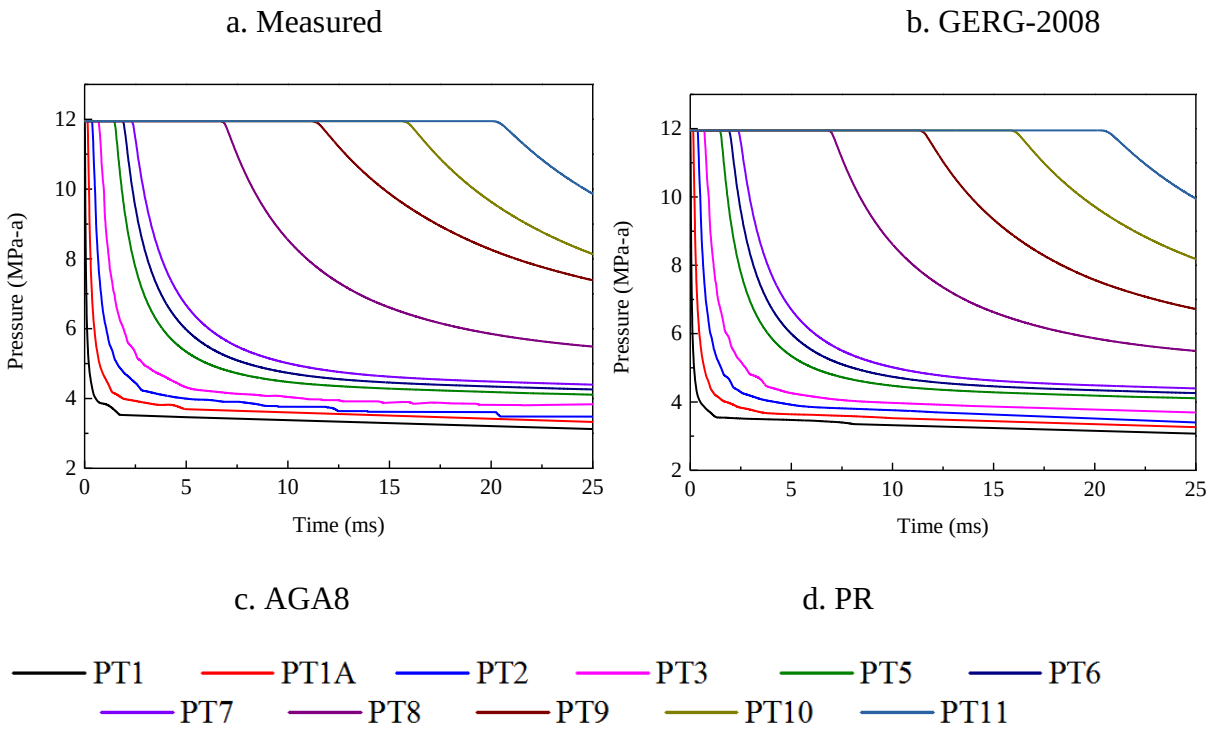

Fig. 4 Measured and simulated pressure using different EOS as a function of time at different locations.

Table 2 The time when the pressure began to decline

	Experiment (ms)	GERG-2008 (ms)	Deviation (%)	PR (ms)	Deviation (%)	AGA8 (ms)	Deviation (%)
PT1	0.00	0.00	0.00	0.00	0.00	0.00	0.00
PT1a	0.11	0.14	27.91	0.14	23.34	0.14	23.34
PT2	0.37	0.37	0.00	0.36	2.7	0.36	2.7
PT3	0.69	0.70	1.82	0.69	0.36	0.68	1.09
PT5	1.53	1.47	4.13	1.49	2.82	1.45	5.44
PT6	1.95	1.93	1.20	1.92	1.71	1.88	3.76
PT7	2.42	2.38	1.91	2.36	2.73	2.32	4.39
PT8	6.99	6.84	2.25	6.83	2.39	6.73	3.82
PT9	11.56	11.34	1.97	11.32	2.15	11.16	3.53
PT10	16.13	15.83	1.92	15.80	2.10	15.60	3.34
PT11	20.65	20.33	1.59	20.28	1.83	20.04	2.99

Fig. 5 compares the decompression wave speeds predicted by different EOS against measurements. Both in the experiment and simulation, the decompression wave speed was obtained through linear regression of the arrival time of the decompression wave for a given pressure at the first five pressure probe locations: PT1, PT1A, PT1B, PT2 and PT3. It is found that the decompression wave speed reduces nearly linearly with the reduction of the pressure during the depressurisation. Overall, the predicted decompression wave speeds are in very good agreement with experimental measurements. Notably, the decompression wave speed curves do not show a pressure plateau. This is because the decompression path (*P*-*T* path) for the given initial pressure and temperature did not intersect with the phase envelope, as shown in Fig. 6, indicating that the mixture did not get into the two-phase region. It also can be seen that the decompression wave speed obtained by AGA8 and GERG-2008 are in better agreement with the measurements.

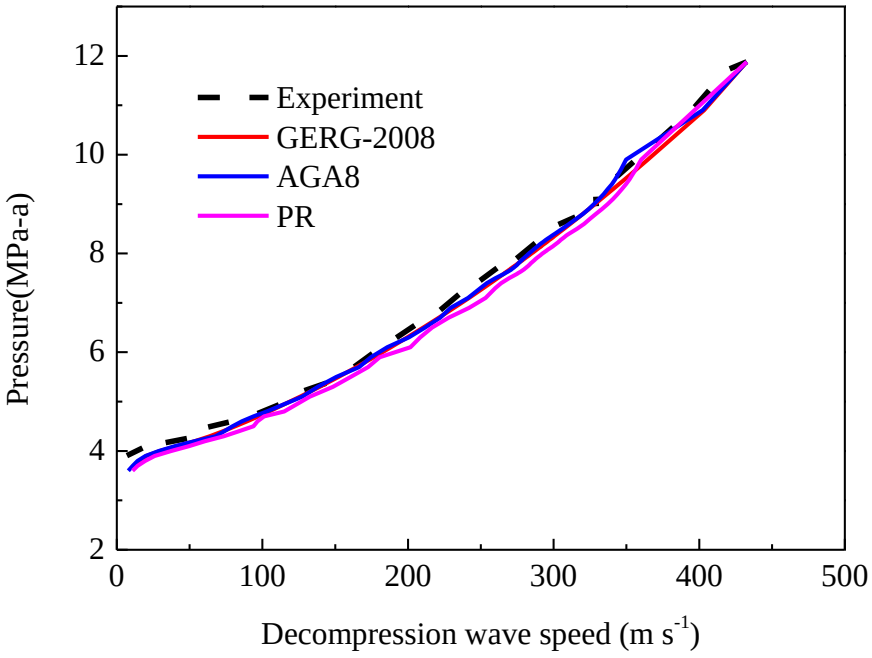

Fig. 5 Decompression wave speed: measured vs predicted by different EOS

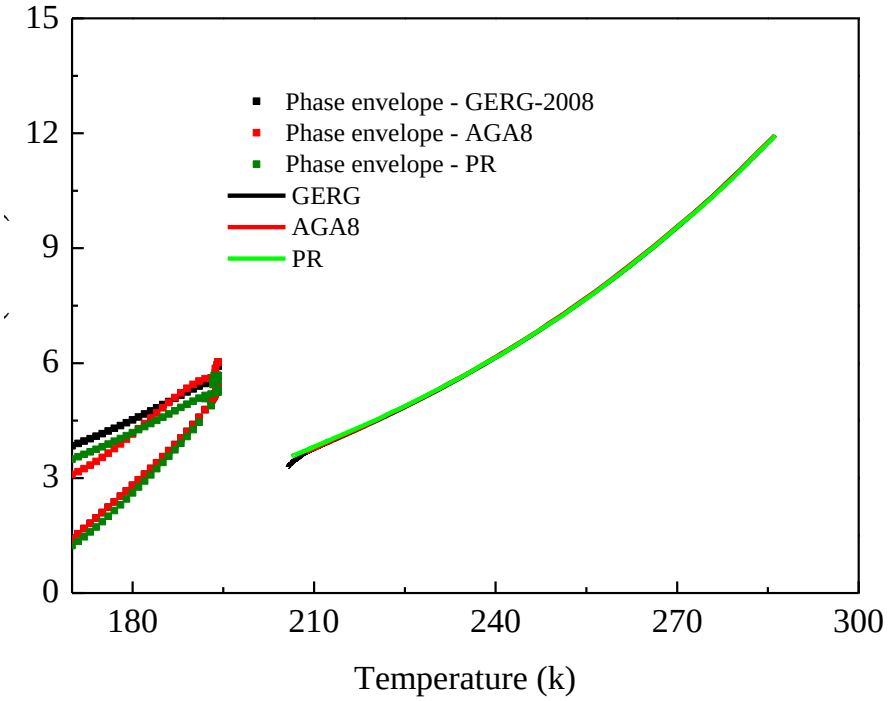

Fig. 6 The *P-T* curve (thermodynamic trajectory) during decompression

3.2. Influence of H_2 fraction on the decompression wave speed

The effect of the H_2 fraction on the decompression wave speed of the H2NG mixture was also studied by carrying out CFD simulations. The results were compared against experimental data of two other shock tube tests performed by Botros et al. [25].

Firstly, 'Test 2' in Ref. [25] was simulated. The initial pressure and temperature were 12.12 MPa and 287.62 K respectively. The composition of the mixture was 88.61% CH_4, 0.190% C_2H_6, 0.135% C_3H_8, 0.115% CO, 8.280% H_2, 0.585%N_2, and 2.085% CO_2.

Simulations of 4 cases with various H_2 fractions using the same initial pressure and temperature as in the experiment were carried out. The composition for each simulation are presented in Table 3. Case 3 simulates the mixture used in Test 2. In these simulations, the GERG-2008 EOS was used to estimate the physical properties of the H2NG mixtures.

Table 3 Mixture Compositions

Component	Case 1	Case 2	Case 3	Case 4
CH_4	96.890%	94.890%	88.610%	80.890%
C_2H_6	0.190%	0.190%	0.190%	0.190%
C_3H_8	0.135%	0.135%	0.135%	0.135%
CO	0.115%	0.115%	0.115%	0.115%
H_2	0.000%	2.000%	8.280%	16.000%
N_2	0.585%	0.585%	0.585%	0.585%
CO_2	2.085%	2.085%	2.085%	2.085%

Fig.7 shows the decompression wave speed curves predicted for different H_2 fractions. The decompression wave speed measured in Test 2 is also shown. It is shown that the decompression wave speed predicted for Case 3 (solid green line) is in good agreement with that measured in Test 2 (dashed green line).

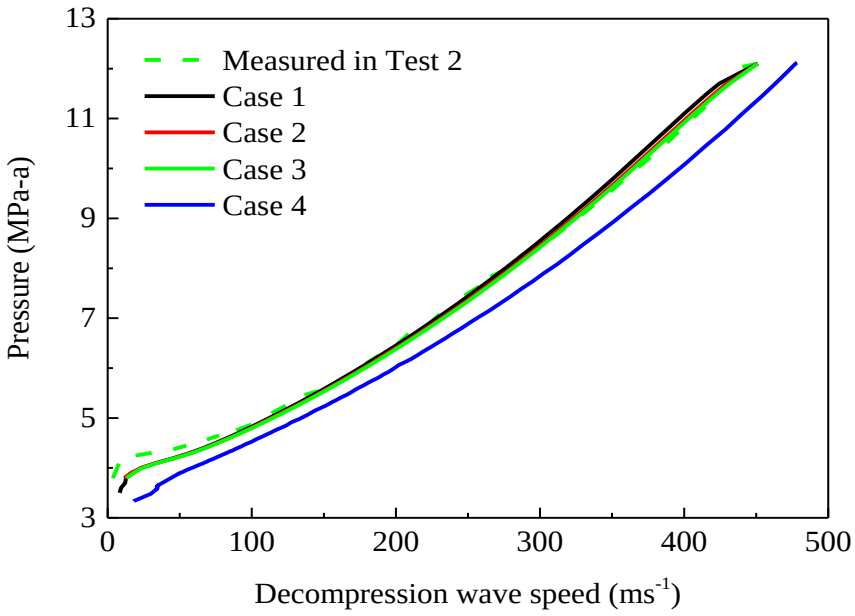

Fig. 7 Decompression wave speeds predicted for different H_2 fractions

It is observed that up to 8% H_2 fraction in the mixture, the decompression wave speed is not significantly affected. Only at higher pressure, a higher H_2 fraction causes a slight right shift of the

decompression wave speed curve. However, further increase in the H_2 fraction to 16% results in a significant right shift of the decompression wave speed curve. Fig. 8 shows the phase envelopes as well as the *P-T* curves during the decompression. Notably, addition of H_2 to NG significantly affect the phase equilibrium of the mixture. However, the thermodynamic trajectories for different H_2 fractions are very close to each other and they all do not intersect with the corresponding phase envelopes. Moreover, it can be seen from Fig. 9, when the H_2 fraction is less than 8%, the effect of the H_2 fraction on the speed of sound in the H2NG mixture is not significant for the initial pressure and temperature given in Test 2. This explains the very small difference in the decompression wave speed when increasing the H_2 fraction up to 8%. When the H_2 fraction reaches 16% (see Fig. 9), the speed of sound of the mixture becomes significantly higher than that of the mixture with 8% H_2. In this case, the decompression wave speed curve shows a right shift.

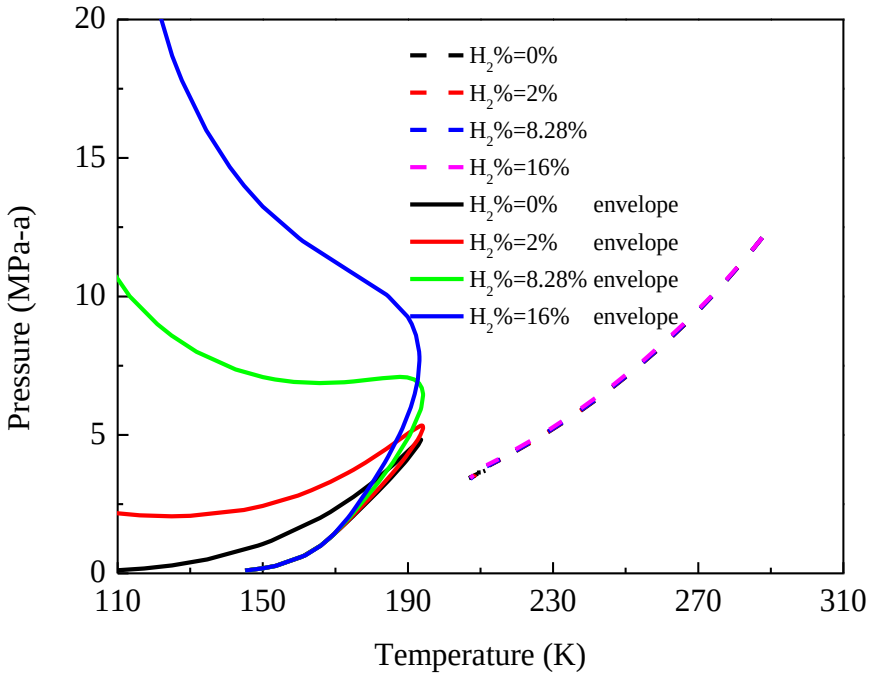

Fig. 8 The *P-T* curve (thermodynamic trajectories) during decompression

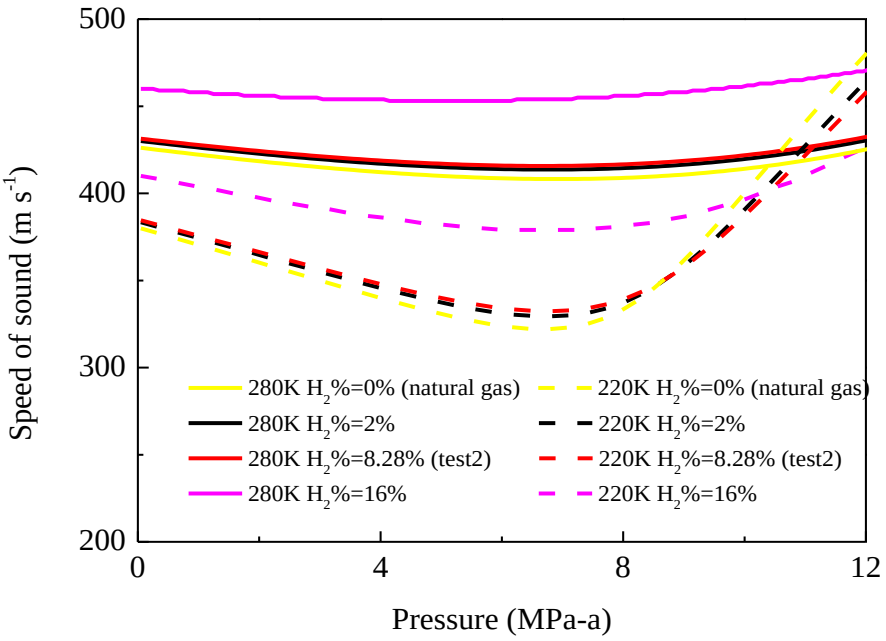

Fig. 9 The speed of sound curves at 280 K and 220 K for different H_2 fractions

Secondly, 'Test 6' in Ref. [10] was also used to investigate the effect of H_2 fraction on the decompression behaviour. In the experiment, the initial pressure and temperature were 21.344 MPa and 287.62 K respectively. The composition of the mixture tested was 79.3017% CH_4, 10.0013% C_2H_6, 6.1103% C_3H_8, 1.3280% i-C_4H_{10}, 1.7365% n-C_4H_{10}, 0.45%N_2, and 1.0723% CO_2.

Based on the mixture used in Test 6, 2% H_2 and 6% H_2 were introduced to the mixture respectively. Three cases were simulated, with mixture compositions shown in Table 4. Case 1 simulates the mixture used in Test 6. As before, the GERG-2008 EOS was used to estimate the thermodynamic properties.

Table 4 Mixture Compositions

component	Case 1	Case 2	Case 3
CH_4	79.30%	77.302%	73.302%
C_2H_6	10.00%	10.00%	10.00%
C_3H_8	6.11%	6.11%	6.11%
i-C_4H_{10}	1.33%	1.33%	1.33%
n-C_4H_{10}	1.74%	1.74%	1.74%
H_2	0.00%	2.00%	6.00%

N_2	0.45%	0.45%	0.45%
CO_2	1.07%	1.07%	1.07%

Fig. 10 shows the decompression wave speed curves for mixtures with different H_2 fractions. The decompression wave speed obtained from Test 6 is also shown. It is found that for Test 6 (dashed black line), the decompression wave speed curve can be broken up into three parts. The first is a rapid drop stage, followed by a second relatively stable plateau stage. This occurs when the decompression path touches the phase boundary (refer to Fig. 11). Subsequently, the pressure drop resumes. It is also found that the proposed model can reasonably well predict the decompression wave speed of NG mixtures when there is phase change involved, not only for the 'rapid drop' stage, but also for the pressure plateau (see the black solid and dashed lines in Fig. 10). The over-prediction of the plateau pressure may be due to delayed bubble formation [52, 53] during the rapid phase change.

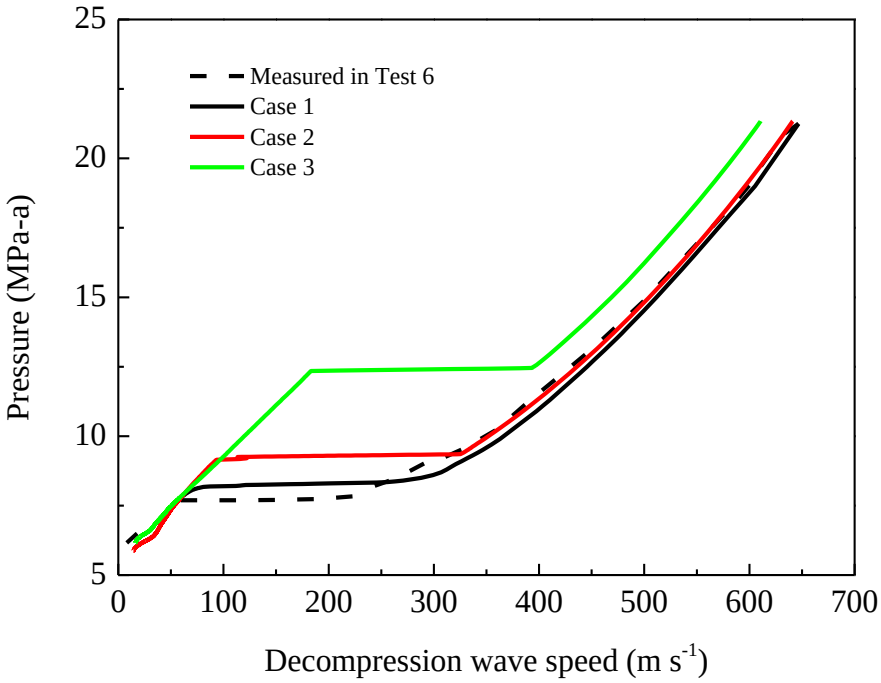

Fig. 10 Decompression wave speeds predicted for mixtures with various H_2 fractions

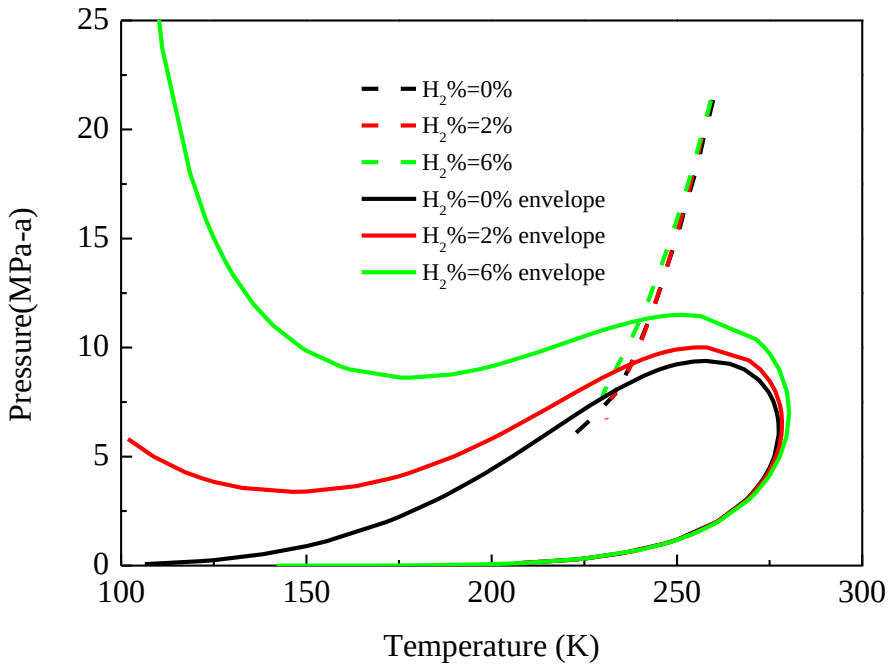

Fig. 11 The *P-T* curve (thermodynamic trajectory) during decompression

In this case, it is found that the H_2 fraction has a much greater influence on the decompression wave speed than that in the former case. Obviously, a relatively small difference in the H_2 fraction results in considerable change in the decompression wave speed. Particularly, increase of H_2 fraction leads to a 'left shift' of the 'rapid drop' part of the curve and a significantly higher plateau pressure. This implies that the required toughness for the pipeline should be much higher. As mentioned above, the H_2 fraction has a very significant effect on the phase envelope. Fig. 11 shows the decompression trajectories as well as the phase envelopes. It is found that in all these cases, the decompression paths intersect with the corresponding phase envelopes. Because adding a small fraction of H_2 to the NG mixture results in significant shift of the bubble line in the phase envelope, the presence of H_2 resulted in a different pressure plateau levels was clearly related to the bubble line of the phase envelope. Therefore, even a relatively lower H_2 fraction will lead to a much higher plateau pressure. Also, the properties of the mixtures change dramatically when the decompression path crosses the phase envelopes.

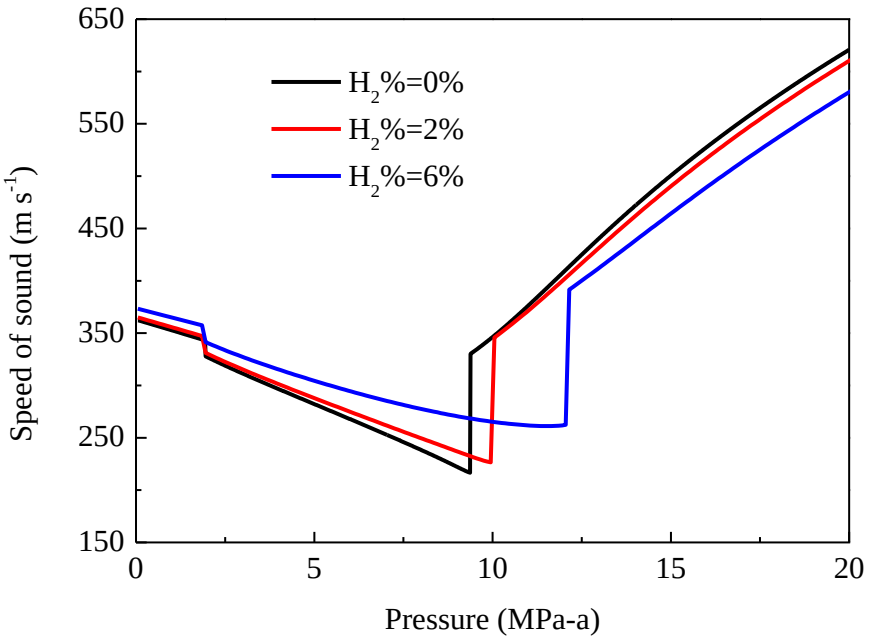

Fig. 12 The pressure vs speed of sound curves at 260 k for different H_2 fractions

Fig. 12 shows the speeds of sound in the mixtures estimated at 260 K. At 20 MPa, the speeds of sound for H_2%=0%, 2% and 8% are around 621, 611 and 581 m s^{-1} respectively. All the speeds of sound decrease gradually with the decrease in pressure. A higher H_2 fraction corresponds to a lower speed of sound. When approaching the phase boundary (also see Fig. 11), the speed of sound is seen to drop dramatically. The points of abrupt change in the speed of sound for different H_2 fractions in the mixture (0%, 2% and 8%) are around 9.4 MPa, 10.1MPa and 12.1 MPa respectively. This is in accordance with the phase envelopes of different mixtures (also see Fig. 11). The great deviation in the speed of sound has a significant effect on the decompression wave speed.

In conjunction with the fracture propagation speed, the predicted decompression wave speed can be used to determine the 'arrest toughness' (C_V), which is the minimum CVN energy required for the pipeline to arrest the running fracture. Table 5 shows basic conditions for the calculation of the fracture propagation speed curve of an 18″ pipeline using X52 or X70 steel.

Table 5 Calculation conditions for fracture propagation speed

Case	Steel grade	Pipe diameter (mm)	Wall thickness (mm)	Yield stress (MPa)
1	X52	457	13.3	359
2	X70	457	9.9	483

Fig.13 and Fig. 14 show the application of BTCM method to determine the arrest toughness. It is clear that the increase of H_2 fraction in the H2NG mixture leads to lower arrest toughness required for the material. For X52 steel, the arrest toughness required for the natural gas and the H2NG (16% H_2) are 21.9 J and 19.7 J respectively, while for X70 steel, they are 35.7 J and 31.9 J respectively. This also indicates that for higher grade steel, higher arrest toughness is required.

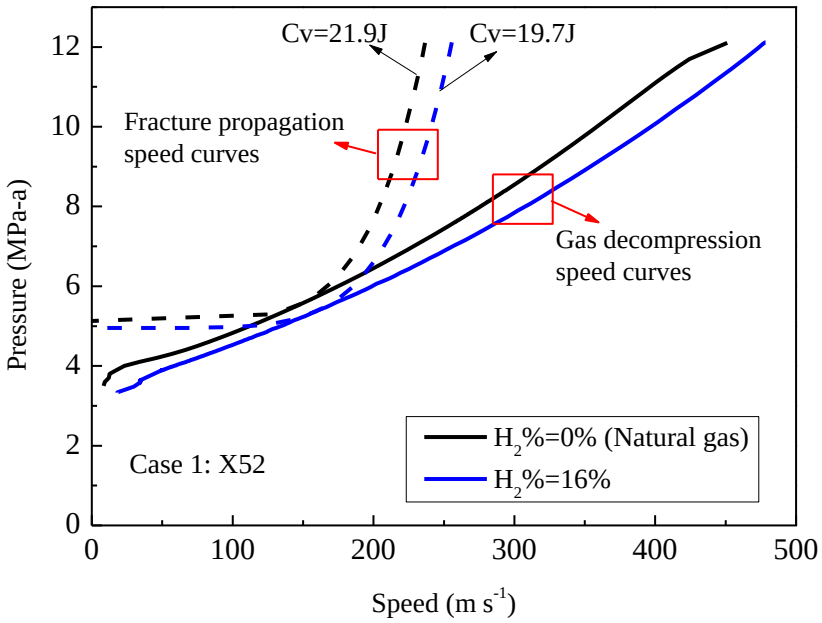

Fig. 13 Predicted decompression curves for NG and a H2NG mixture with 16% H_2, and fracture propagation speed curves for the 18″ pipeline using X52 steel.

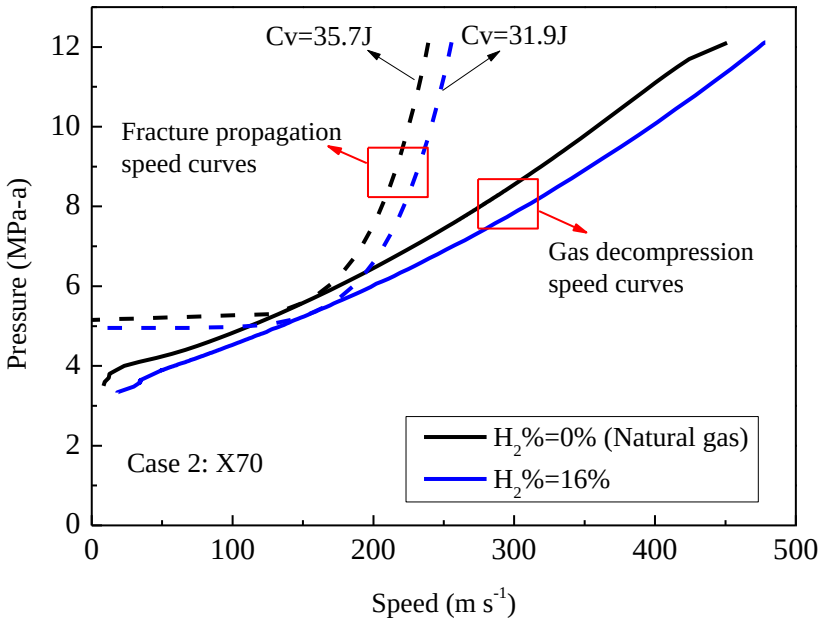

Fig. 14 Predicted decompression curves for NG and a H2NG mixture with 16% H_2, and fracture propagation speed curves for the 18″ pipeline using X70 steel.

4. Conclusions

In this paper, a CFD model is proposed for the prediction of the decompression behaviour of high-pressure H2NG mixtures in pipelines. Three EOS (PR, AGA8 and GERG-2008) were incorporated into the CFD code using a 'real gas' model to evaluate their ability to predict the decompression wave speed. It was found that the time-varying pressure and decompression wave speeds predicted by all three EOS were in satisfactory agreement with the measurements from shock tube tests. Notably, the prediction based on the GERG-2008 EOS showed the best agreement with the experimental data. Also, the thermodynamic trajectories (decompression paths) obtained by the three EOS were almost identical. Therefore, all the three EOS are acceptable in the prediction of the decompression wave speed of H2NG pipelines. The GERG-2008 EOS is recommended as it outperforms the other two EOS in terms of the prediction of decompression wave speed.

The influence of the H_2 fraction in the H2NG mixture on decompression wave speed was investigated using the proposed model using the GERG-2008 EOS by simulating two experiments. Good agreement was obtained between simulation results and experimental measurements. It was found that the effect of H_2 fraction on the decompression wave speed were quite different for the two cases, depending on whether the thermodynamic trajectory intersects with the corresponding phase envelope or not. In general, if the thermodynamic trajectory does not cross the phase boundary, the variation of H_2 fraction (from 0% to 10%) has only a limited effect on the decompression wave speed, particularly at high pressures. On the contrary, if the thermodynamic trajectory touches the phase boundary during the depressurisation, higher H_2 fraction can result in a significant shift of the decompression wave speed curve upward and to the left, implying higher plateau pressure.

Overall, this study shows that the proposed CFD model is able to predict the decompression wave speed of H2NG mixtures. This will help the material design of the H2NG pipelines to ensure that the fracture propagation can be arrested in case of an accident. Further studies will be directed to the development of a discharge model for H2NG pipelines using the proposed decompression simulation methods. This will enable more accurate 'consequence modelling' of an H2NG pipeline failure.

References

[1] A. Witkowski, A. Rusin, M. Majkut, and K. Stolecka, "Comprehensive analysis of hydrogen compression and pipeline transportation from thermodynamics and safety aspects," *Energy*.

[2] E. Polman *et al.*, "Reduction of CO2 emissions by adding hydrogen to natural gas," GASTEC Technology BV, Apeldoorn, Apeldoorn, The Netherlands2003.

[3] F. Tabkhi, C. Azzaro-Pantel, L. Pibouleau, and S. Domenech, "A mathematical framework for modelling and evaluating natural gas pipeline networks under hydrogen injection," *International Journal of Hydrogen Energy,* vol. 33, no. 21, pp. 6222-6231, 2008/11/01/ 2008.

[4] M. Deymi-Dashtebayaz, A. Ebrahimi-Moghadam, S. I. Pishbin, and M. Pourramezan, "Investigating the effect of hydrogen injection on natural gas thermo-physical properties with various compositions," *Energy,* vol. 167, pp. 235-245, 2019/01/15/ 2019.

[5] B. Wang, Y. Liang, J. Zheng, R. Qiu, M. Yuan, and H. Zhang, "An MILP model for the reformation of natural gas pipeline networks with hydrogen injection," *International Journal of Hydrogen Energy,* vol. 43, no. 33, pp. 16141-16153, 2018/08/16/ 2018.

[6] B. Fan *et al.*, "Effect of hydrogen injection strategies on mixture formation and combustion process in a hydrogen direct injection plus natural gas port injection rotary engine," *Energy Conversion and Management,* vol. 160, pp. 150-164, 2018/03/15/ 2018.

[7] B. Fan *et al.*, "The influence of hydrogen injection strategy on mixture formation and combustion process in a port injection (PI) rotary engine fueled with natural gas/hydrogen blends," *Energy Conversion and Management,* vol. 173, pp. 527-538, 2018/10/01/ 2018.
[8] J. Zareei, A. Rohani, and W. M. F. Wan Mahmood, "Simulation of a hydrogen/natural gas engine and modelling of engine operating parameters," *International Journal of Hydrogen Energy,* vol. 43, no. 25, pp. 11639-11651, 2018/06/21/ 2018.
[9] M. Capocelli and M. De Falco, "Enriched Methane: A Ready Solution for the Transition Towards the Hydrogen Economy," in *Enriched Methane: The First Step Towards the Hydrogen Economy*, M. De Falco and A. Basile, Eds. Cham: Springer International Publishing, 2016, pp. 1-21.
[10] K. K. Botros, J. Geerligs, L. Fletcher, B. Rothwell, P. Venton, and L. Carlson, "Effects of Pipe Internal Surface Roughness on Decompression Wave Speed in Natural Gas Mixtures," no. 44212, pp. 907-922, 2010.
[11] K. K. Botros, J. Geerligs, J. Zhou, and A. Glover, "Measurements of flow parameters and decompression wave speed following rupture of rich gas pipelines, and comparison with GASDECOM," *International Journal of Pressure Vessels and Piping,* vol. 84, no. 6, pp. 358-367, 6// 2007.
[12] E. Burlutskiy, "Mathematical modelling on rapid decompression in base natural gas mixtures under rupturing," *Chemical Engineering Research and Design,* vol. 91, no. 1, pp. 63-69, 1// 2013.
[13] E. Burlutskiy, "A one-dimensional mathematical model of multi-component fluid flow in pipes and its application to rapid decompression in dry natural gas mixtures," *International Journal of Pressure Vessels and Piping,* vol. 104, pp. 30-36, 4// 2013.
[14] E. Burlutskiy, "Numerical analysis of phase behavior during rapid decompression of rich natural gases," *Process Safety and Environmental Protection,* vol. 92, no. 6, pp. 555-564, 11// 2014.
[15] R. P. Cleaver and A. R. Halford, "A model for the initial stages following the rupture of a natural gas transmission pipeline," *Process Safety and Environmental Protection,* vol. 95, pp. 202-214, 5// 2015.
[16] A. Elshahomi, C. Lu, G. Michal, X. Liu, A. Godbole, and P. Venton, "Decompression wave speed in CO2 mixtures: CFD modelling with the GERG-2008 equation of state," *Applied Energy,* vol. 140, pp. 20-32, 2/15/ 2015.
[17] A. Wells, "Fracture control: Past, present and future," (in English), *Experimental Mechanics,* vol. 13, no. 10, pp. 401-410, 1973/10/01 1973.
[18] B. Eiber, L. Carlson, B. Leis, and A. Gilroy-Scott. (1999) Full-scale tests confirm pipe toughness for North American pipeline. *Oil & Gas Journal*. 48-48-54. Available: http://search.proquest.com/docview/274384872?accountid=15112
[19] G. D. Fearnehough, "Fracture propagation control in gas pipelines: A survey of relevant studies," *International Journal of Pressure Vessels and Piping,* doi: 10.1016/0308-0161(74)90007-6 vol. 2, no. 4, pp. 257-282, 1974.
[20] T. K. Groves, P. R. Bishnoi, and J. M. E. W. allbridge, "Decompression Wave Velocities In Natural Gases In Pipe Lines," *Canadian Journal of Chemical Engineering,* vol. 56, no. 1, pp. 664-668, 1978.
[21] A. B. Rothwell, "Fracture propagation control for gas pipelines—past, present and future," *In: Denys R, editor. Proceedings of the 3rd International Pipeline Technology Conference,* vol. 1, pp. 387–405, 2000.
[22] D. Rudland *et al.*, "FIRST MAJOR IMPROVEMENTS TO THE TWO CURVE DUCTILE FRACTURE MODEL PART I MAIN BODY," U.S. Department of Transportation Research and Special Programs Administration Washington DC 20590 and Pipeline Research Council International, Inc. Arlington, VA 222092007.
[23] K. K. Botros, L. Carlson, and M. Reed, "Extension of the semi-empirical correlation for the effects of pipe diameter and internal surface roughness on the decompression wave speed to include High Heating Value Processed Gas mixtures," *International Journal of Pressure Vessels and Piping,* vol. 107, pp. 12-19, 7// 2013.
[24] K. K. Botros, J. Geerligs, B. Rothwell, L. Carlson, L. Fletcher, and P. Venton, "Transferability of decompression wave speed measured by a small-diameter shock tube to full size pipelines and

implications for determining required fracture propagation resistance," *International Journal of Pressure Vessels and Piping,* vol. 87, no. 12, pp. 681-695, 12// 2010.
[25] K. K. Botros, S. Igi, and J. Kondo, "Measurements of Decompression Wave Speed in Natural Gas Containing 2-8% (Mole) Hydrogen by a Specialized Shock Tube," no. 50275, p. V003T05A001, 2016.
[26] A. Cosham, R. J. Eiber, and E. B. Clark, "GASDECOM: Carbon Dioxide and Other Components," no. 44212, pp. 777-794, 2010.
[27] A. Cosham, D. G. Jones, K. Armstrong, D. Allason, and J. Barnett, "The Decompression Behaviour of Carbon Dioxide in the Dense Phase," no. 45141, pp. 447-464, 2012.
[28] (2002). *Gas decompression behavior following the rupture of high pressure pipelines - Phase 1, PRCI Contract PR-273-0135.*
[29] A. Cosham, D. G. Jones, K. Armstrong, D. Allason, and J. Barnett, "The Decompression Behaviour of Carbon Dioxide in the Dense Phase," in *Proceedings of the 2012 9th International Pipeline Conference*, Calgary, Alberta, Canada, 2012.
[30] C. Lu *et al.*, "INVESTIGATION OF THE EFFECTS OF PIPE WALL ROUGHNESS AND PIPE DIAMETER ON THE DECOMPRESSION WAVE SPEED IN NATURAL GAS PIPELINES," in *Proceedings of the 2012 9th International Pipeline Conference*, Calgary, Alberta, Canada, 2012.
[31] D. G. Jones and D. W. Gough, "Rich Gas Decompression Behaviour in Pipelines," presented at the AGA-EPRG Linepipe Research Seminar IV, Duisburg, 22-24 September 1981, 1981.
[32] D. J. Picard and P. R. Bishnoi, "The Importance of Real-Fluid Behavior and Nonisentropic Effects in Modeling Decompression Characteristics of Pipeline Fluids for Application in Ductile Fracture Propagation Analysis," *THE CANADIAN JOURNAL OF CHEMICAL ENGINEERING,* vol. 66, no. 1, pp. 3-12, 1988.
[33] D. J. Picard and P. R. Bishnoi, "The Importance of Real-Fluid Behavior in Predicting Release Rates Resulting From High-Pressure Sour-Gas Pipeline Ruptures," *THE CANADIAN JOURNAL OF CHEMICAL ENGINEERING,* vol. 67, no. 1, pp. 3-9, 1989.
[34] H. Mahgerefteh, S. Brown, and G. Denton, "Modelling the impact of stream impurities on ductile fractures in CO2 pipelines," *Chemical Engineering Science,* vol. 74, pp. 200-210, 5/28/ 2012.
[35] H. Mahgerefteh, S. Brown, and S. Martynov, "A study of the effects of friction, heat transfer, and stream impurities on the decompression behavior in CO2 pipelines," *Greenhouse Gases: Science and Technology,* vol. 2, no. 5, pp. 369-379, 2012.
[36] H. E. Jie, B. P. Xu, J. X. Wen, R. Cooper, and J. Barnett, "Predicting The Decompression Characteristics of Carbon Dioxide Using Computational Fluid Dynamics," in *Proceedings of the 2012 9th International Pipeline Conference*, Calgary, Alberta, Canada 2012, p. 11: ASME.
[37] H. Li and J. Yan, "Evaluating cubic equations of state for calculation of vapor–liquid equilibrium of CO2 and CO2-mixtures for CO2 capture and storage processes," *Applied Energy,* vol. 86, no. 6, pp. 826-836, 6// 2009.
[38] K. K. Botros, "Measurements of Speed of Sound in Lean and Rich Natural Gas Mixtures at Pressures up to 37 MPa Using a Specialized Rupture Tube," *International Journal of Thermophysics,* journal article vol. 31, no. 11, pp. 2086-2102, December 01 2010.
[39] http://www.truboprovod.ru/news/big_news/en_ntp_has_licensed_gerg.shtml.
[40] K. E. Starling and J. L. Savidge, *Compressibility Factors of Natural Gas and Other Related Hydrocarbon Gases*. AGA, American Gas Association, 1994.
[41] S. W. Hopke and L. C.J, "Application of BWRS Equation to Natural Gas Systems," presented at the 76'h National AIChE Meeting, American Institute of Chemical Engineers, Tulsa, Oklahoma, USA, 1974.
[42] D. Y. Peng and D. B. Robinson, "A new two constants equation of state," *Industrial Engineering and Chemical Fundamentals,* vol. 15, p. 59, 1976.
[43] G. Soave, "Equilibrium constants from a modified Redlich-Kwong equation of state," *Chemical Engineering Science,* vol. 27, no. 6, pp. 1197-1203, 1972.

[44] R. Span and W. Wagner, "A New Equation of State for Carbon Dioxide Covering the Fluid Region from the Triple-Point Temperature to 1100 K at Pressures up to 800 MPa," *Journal of Physical and Chemical Reference Data,* vol. 25, no. 6, pp. 1509-1596, 1996.
[45] K. K. Botros, J. Geerligs, B. Rothwell, and T. Robinson, "Measurements of Decompression Wave Speed in Pure Carbon Dioxide and Comparison With Predictions by Equation of State," *Journal of Pressure Vessel Technology,* vol. 138, no. 3, pp. 031302-031302-8, 2015.
[46] K. K. Botros, J. Geerligs, B. Rothwell, and T. Robinson, "Measurements of Decompression Wave Speed in Binary Mixtures of Carbon Dioxide and Impurities," *Journal of Pressure Vessel Technology,* vol. 139, no. 2, pp. 021301-021301-11, 2016.
[47] K. K. Botros, J. Geerligs, B. Rothwell, and T. Robinson, "Measurements of Decompression Wave Speed in Simulated Anthropogenic Carbon Dioxide Mixtures Containing Hydrogen," *Journal of Pressure Vessel Technology,* vol. 139, no. 2, pp. 021201-021201-7, 2016.
[48] M. Richter, M. A. Ben Souissi, R. Span, and P. Schley, "Accurate (p, ρ, T, x) Measurements of Hydrogen-Enriched Natural-Gas Mixtures at T = (273.15, 283.15, and 293.15) K with Pressures up to 8 MPa," *Journal of Chemical & Engineering Data,* vol. 59, no. 6, pp. 2021-2029, 2014/06/12 2014.
[49] R. Hernández-Gómez, D. Tuma, D. Lozano-Martín, and C. R. Chamorro, "Accurate experimental (p, ρ, T) data of natural gas mixtures for the assessment of reference equations of state when dealing with hydrogen-enriched natural gas," *International Journal of Hydrogen Energy,* vol. 43, no. 49, pp. 21983-21998, 2018/12/06/ 2018.
[50] G. Xia, D. Li, and C. L. Merkle, "Consistent properties reconstruction on adaptive Cartesian meshes for complex fluids computations," *Journal of Computational Physics,* vol. 225, no. 1, pp. 1175-1197, 7/1/ 2007.
[51] S. R. Hanna, R. Britter, and P. Franzese, "A baseline urban dispersion model evaluated with Salt Lake City and Los Angeles tracer data.," *Atmospheric Environment,* vol. 37, pp. 5069-5082, 2003.
[52] B. Liu, X. Liu, C. Lu, A. Godbole, G. Michal, and A. K. Tieu, "A CFD decompression model for CO2 mixture and the influence of non-equilibrium phase transition," *Applied Energy*.
[53] B. Liu, X. Liu, C. Lu, A. Godbole, G. Michal, and A. K. Tieu, "Decompression Modelling of Pipelines Carrying CO2-N2 Mixture and the Influence of Non-equilibrium Phase Transition," *Energy Procedia,* vol. 105, pp. 4204-4209, 5// 2017.